Elsevier Editorial System(tm) for Applied Catalysis A
Manuscript Draft

Title: Platinum supported on highly-dispersed ceria on activated carbon for the total oxidation of VOCs
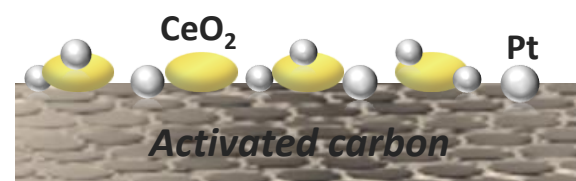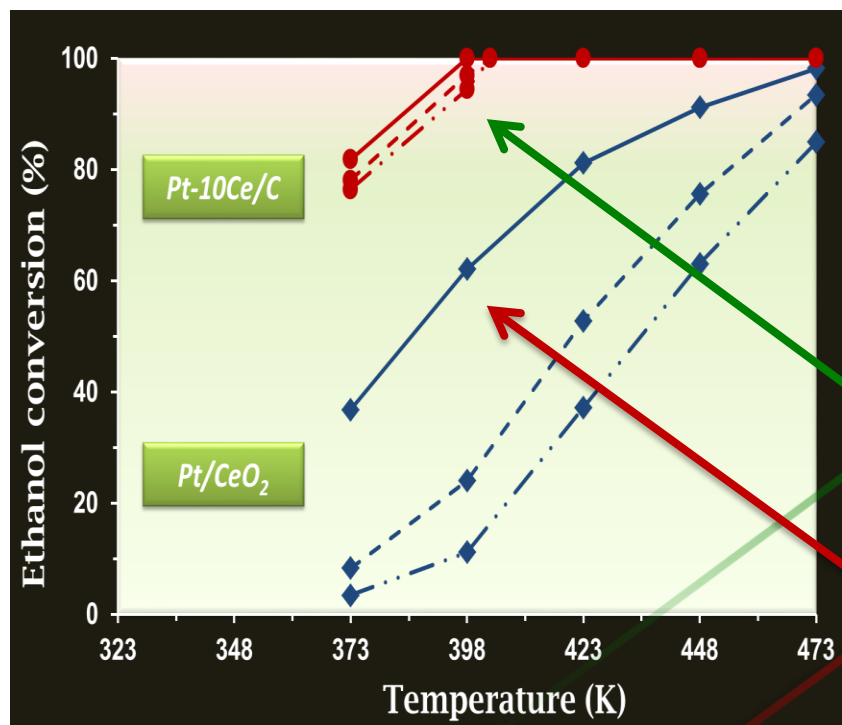
Article Type: Research Paper

Corresponding Author: Prof. Antonio Sepúlveda-Escribano, PhD

Corresponding Author's Institution: University of Alicante

First Author: Zinab Abdelouahab-Reddam

Order of Authors: Zinab Abdelouahab-Reddam; Rachad El Mail; Fernando Coloma-Pascual; Antonio Sepúlveda-Escribano, PhD

Highlights

- Pt-CeO$_2$ catalysts supported on activated carbon are active in the total oxidation of VOCs.
- These catalysts have shown higher activity than platinum supported on bulk ceria.
- The best catalyst contained only 10wt% ceria.
- Pt-10Ce/C catalyst showed a high stability under both dry and humid conditions.

Platinum supported on highly-dispersed ceria on activated carbon for the total oxidation of VOCs

Z. Abdelouahab-Reddam[1,2], R. El Mail[2], F.Colomal[1], A. Sepúlveda-Escribano[1]

(1) Laboratorio de Materiales Avanzados, Departamento de Química Inorgánica - Instituto Universitario de Materiales de Alicante, Universidad de Alicante, Ap. 99, E-03080, Alicante, Spain.

(2) Equipe de Recherche Chimie de l'Eau et Pollution Atmosphérique, Département de Chimie, Faculté des Sciences, Université Abdelmalek Essaadi, Tétouan, Morocco.

Abstract

Catalysts consisting in platinum supported on cerium oxide highly dispersed on activated carbon, with a Pt loading of 1 wt.% and ceria loadings of 5, 10 and 20 wt.% have been prepared by impregnation method and characterized by several techniques (N_2 adsorption at 77 K, ICP, XRD, H_2-TPR and XPS). Their catalytic behavior has been evaluated in the total oxidation of ethanol and toluene after reduction at 473 K. The obtained results show that the prepared catalysts have better performances than platinum supported on bulk CeO_2. The best catalytic performance was obtained for 10 wt.% ceria loading, likely due to an optimum synergistic interaction between highly dispersed cerium oxide and platinum particles. Pt-10Ce/C achieves total conversion of ethanol and toluene to CO_2 at 433 K and 453 K, respectively, and shows no deactivation during a test for 100 h. Under humid conditions (relative humidity, RH, of 40 and 80 %), the activity was only slightly influenced due to the hydrophobic character of the activated carbon support, which prevents the adsorption of water.

Keywords: Pt; Ceria; Activated carbon; VOCs; Total combustion

1. Introduction

Volatile organic compounds (VOCs) are known as one of the most important class of air pollutants. Different human activities produce the emission of VOCs to the atmosphere, including transport and the use of solvents in several industries [1]. These compounds cause several health problems, ranging from simple discomfort like eyes and respiratory tract irritation to serious complications such as damage to liver and kidney and alterations in central nervous system and, further, some of them can cause

1

cancer after prolonged exposure [2,3]. Besides, VOCs play a key role on the process of formation of photochemical smog [4,5]. Catalytic oxidation is one of the most promising technologies for their abatement [6,7]. This technique reaches high efficiency at low temperatures, obtaining considerable environment and economic benefits [8]. The most commonly used catalysts in VOCs oxidation are supported noble metals (Pt, Pd, Rh, Au, etc) and metal oxides (CeO_2, CuO, MnO_x, CoO_x, etc.) [9-14]. Among the catalysts based on metal oxides which are studied in the literature, cerium oxide is considered to be particularly suitable for total oxidation of VOCs, either pure or in combination with noble metals or other metal oxides [15-19]. The high activity of ceria in total oxidation reactions is ascribed to its high oxygen storage capacity (OSC) and its exceptional redox properties [20]. The beneficial effect due to the addition of a noble metal to the ceria-based catalysts has been demonstrated in the literature [21,22]. Thus, noble metals improve the reducibility of ceria through the establishment of a metal-oxide interaction, which weakens the Ce−O bonds located at the interface Pt−CeO_2 and, consequently, increases the mobility of lattice oxygen involved in VOCs oxidation through a Mars-van Krevelen reaction mechanism [16]. On the other hand, the efficiency of ceria-based catalysts in the total oxidation of VOCs can be improved by using an appropriate support as activated carbon. In fact, dispersion of ceria on a support with a high surface area such as activated carbon could lead to a most efficient catalyst, which provides more active sites available for the reaction with a lower cost with respect to bulk ceria catalysts. Moreover, activated carbon is a suitable support for catalysts destined to the complete oxidation of VOCs due to its hydrophobic character. In fact, the water vapour generated upon VOCs oxidation can deactivate the active sites of the supports, which show a hydrophilic behaviour, mainly at low temperatures. Additionally, ambient air usually contains water molecules, which should negatively affect the catalytic activity [23]. In this sense, the objective of the present paper is to prepare platinum catalysts supported on highly dispersed ceria on activated carbon, with different ceria loadings, in order to determine the effect of the oxide content on the catalytic activity in the total oxidation of ethanol and toluene, selected as representative molecules of VOCs.

2. Experimental

2.1. Preparation of catalysts

Highly dispersed ceria on activated carbon (xCe-C supports, where x is the ceria loading) have been prepared by impregnation with excess of solvent. A commercial activated carbon (Nuchar RGC 30, from Mead Westvaco) referred as "C" was impregnated with acetone solutions containing the appropriate amounts of the Ce precursor ($Ce(NO_3)_3 \cdot 6H_2O$) to obtain an oxide loading of 5, 10 and 20 wt.%. Excess of solvent was removed by flowing nitrogen through the slurries at room temperature, and then the solid samples were dried during 12 h at 383 K, and treated under a helium flow (50 mL·min^{-1}) at 623 K for 5 h, with a heating rate of 1 K·min^{-1}, with the purpose to decompose the cerium precursor and to obtain CeO_2 [24]. For the sake of comparison, a bulk ceria (CeO_2) support was prepared by precipitation from an aqueous solution of $Ce(NO_3)_3 \cdot 6H_2O$ containing an excess of urea. The solution was heated at 353-363 K and kept under stirring during 8 h to facilitate urea decomposition. Then, a few drops of concentrated ammonia solution were added slowly with stirring to ensure complete precipitation. The suspension was then cooled down to room temperature, filtered and washed with ultrapure water. Resulting solids were dried at 383 K for 12 h, and finally calcined at 673 K for 4 h, with a heating rate of 3K·min^{-1}.

Catalysts were prepared by the impregnation of the previously obtained supports with an acetone solution of the Pt precursor ($H_2PtCl_6 \cdot 6H_2O$) with the appropriate concentration to obtain 1 wt.% Pt. After 24 h, the solvent excess was removed under vacuum at room temperature in a rotary evaporator. The obtained catalysts were dried during 12 h at 383 K and labeled by adding Pt/ to the nomenclature used for the corresponding supports.

2.2. Characterization of catalysts

Textural properties of the supports have been determined by N_2 adsorption at 77 K, on a home-designed and made fully automated manometric equipment. Previous to measurements, samples were out-gassed under vacuum ($<10^{-5}$ Pa) at 523 K for 4 h. Specific surface area, S_{BET}, was calculated using the BET method. Micropore volume, V_0, was calculated by application of the Dubinin–Radushkevich (DR) equation. Volume of mesopores, V_{meso}, was obtained by subtracting the volume of micropores V_0 from the total, estimated by the uptake at a relative pressure of 0.95.

The actual metal content on the catalysts was determined by ICP-OES analysis with a Perkin-Elmer 7300DV spectrometer. Previous to the experiments, the metal was

extracted from the catalysts by burning out the carbon support and then refluxing the ashes in aqua regia for 8 hours.

X-ray powder diffraction patterns of the samples were recorded on a JSO-Debyeflex 2002 system, from Seifert, fitted with a Cu cathode and a Ni filter, using a $20°·min^{-1}$ scanning rate. The average crystal size for CeO_2 was estimated by application of the Scherrer equation to the (111) ceria diffraction peak.

Temperature-programmed reduction (TPR) measurements were carried out in a home-made gas flow system using an U-shaped quartz reactor, using a $5\%H_2$/He gas flow of 50 mL·min^{-1} and about 100 mg of catalyst. The temperature was raised at 10 K·min^{-1} from room temperature to 1273 K. Hydrogen consumption was followed by online mass spectrometry (Omnistar, Pfeiffer).

X-Ray photoelectron spectroscopy was performed with a K-ALPHA spectrometer (Thermo Scientific). All spectra were collected using Al-K$_\alpha$ radiation (1486.6 eV), monochromatized by a twin crystal monochromator, yielding a focused X-ray spot with a diameter of 400 µm, at 3 mA × 12 kV. The alpha hemispherical analyser was operated at the constant energy mode with survey scan pass energies of 200 eV to measure the whole energy band and 50 eV in a narrow scan to selectively measure the particular elements. Charge compensation was achieved with the system flood gun that provides low energy electrons and low energy argon ions from a single source. The powder samples were pressed and mounted on the sample holder and placed in the vacuum chamber. Before recording the spectrum, the samples were maintained in the analysis chamber until a residual pressure of *ca.* $5 × 10^{-7}$ N·m^{-2} was reached. The quantitative analysis were estimated by calculating the integral of each peak, after subtracting the S-shaped background, and by fitting the experimental curve to a combination of Lorentzian (30%) and Gaussian (70%) lines. Reduction of the samples were carried out "ex situ" in an U-shaped quartz reactor under flowing hydrogen (50 mL·min^{-1}) at 473 K for 1 h and introduced in an octane solution (in inert atmosphere). Suspensions were evaporated in the XPS system under vacuum conditions.

2.3. Catalytic tests

Three catalytic tests have been used to determine the behaviour of the prepared samples: toluene hydrogenation and the catalytic combustion of ethanol and toluene, selected as probe molecules of VOCs.

Toluene hydrogenation has been used as a tool to estimate differences in the metal dispersion of the prepared catalysts. The use of this reaction is justified by its structure-insensitive character, which makes the catalytic activity to only depend on the amount of metallic sites available at the catalyst surface. Toluene hydrogenation tests were performed in a U-shape quartz reactor at atmospheric pressure, and the products were monitored by on-line gas chromatograph (Agilent 6890N) with a flame ionization detector and HP-Plot/Q (30 m x 0.53 mm) column. Prior to reaction, the samples (100 mg of catalyst diluted in SiC to a total volume of 1.5 mL) were reduced in situ at 473 and 773 K for 2 h under flowing hydrogen (50 mL·min^{-1}) and then cooled under hydrogen to the reaction temperature (333 K). Then, a reaction mixture with a total flow of 50 mL·min^{-1} containing hydrogen and toluene in a H_2/C_7H_8 ratio of 36, obtained by passing the hydrogen flow through a thermostabilized saturator containing toluene at 293 K, was fed to the catalyst.

The experiments of total oxidation of ethanol and toluene were carried out in a U-shape quartz reactor operating in continuous mode, using 150 mg of catalyst diluted in SiC to a total volume of 1.5 mL. Previous to reaction, the catalysts were reduced in situ under flowing hydrogen (50 mL·min^{-1}) at 473 K for 1 h, at a heating rate of 2 K·min^{-1}. At the end of the reduction treatment, H_2 was replaced by He at the same temperature during 1 h and the catalyst was cooled to the reaction temperature under He flow. Catalytic activity was evaluated in the temperature range 323-523 K under atmospheric pressure using a reaction mixture containing 1000 ppm of VOC in air flow of 100 mL·min^{-1}. Reaction products were determined with an on-line gas chromatograph (Agilent 6890N) equipped with a flame ionization detector and HP-Plot/Q (30 m x 0.53 mm) column. An on-line IR detector (SENSOTRAN IR) was also employed for the quantitative analysis of CO_2. In humid condition, distilled water was injected by a Gilson 307 HPLC pump and evaporated in a heat box, operating at 473 K. All gas lines of the reaction system were heated to 383 K in order to avoid ethanol, toluene and water adsorption and condensation on tube walls.

3. Results and discussion

3.1. Characterization

3.1.1. N$_2$ adsorption

The nitrogen adsorption-desorption isotherms for the original activated carbon and the carbonaceous supports (not shown) correspond to a mixed Type I and IV

isotherms. They have a large adsorption capacity at low relative pressures, what is characteristic of microporous materials, together with a hysteresis loop at high relative pressures that indicates the presence of a certain proportion of mesoporosity. The textural properties obtained from these isotherms and from the one corresponding to with bulk CeO_2 are shown in Table 1. In the case of carbon-based supports, the BET surface areas decrease with increasing the oxide loading. This reduction is accompanied, as expected, with a decrease in the micro and mesopores volumes, due to the partial blockage of the porosity by ceria crystallites. Moreover, the introduction of the oxide leads to a reduction of activated carbon mass in the sample, which implies an additional negative effect on the porosity since ceria provides lower surface area than the same mass of activated carbon, as can be seen in Table 1. Impregnation with the platinum precursor did not affect the porous texture of the supports.

3.1.2. ICP-OES

Ceria and platinum loadings of the prepared catalysts, determined by ICP-OES, are summarized in Table 2. It can be seen that the nominal and actual platinum loadings are similar for all the catalysts. However, the measured loading of ceria in the supported catalysts is lower than the nominal values, what indicates that some amount of the ceria precursor was lost during the impregnation process and therefore, it was not incorporated to the support. The difference between the actual and the nominal CeO_2 contents increases with oxide loading, maintaining a good correlation between both values.

3.1.3. X-ray diffraction

Fig. 1 shows the X-ray diffraction patterns of Pt/Ce-C catalysts with 5, 10, 20 wt.% ceria loading, together with that of Pt/CeO$_2$. All the profiles show four diffraction peaks, at 28.5º, 33º, 47.5º and 56.3º, corresponding to fluorite phase of ceria (JCPDS 34-394). Moreover, the sample with low content on ceria (Pt/5Ce-C) exhibits two broad peaks at approximately 25º and 44º characteristic of amorphous carbonaceous materials (JCPDS 75-1621). As can be seen, the Pt/CeO$_2$ pattern shows intense and well defined diffraction peaks, while the carbon-supported catalysts present broad peaks, whose intensities rise with the increase of ceria loading. This indicates the presence of small particles of CeO_2 highly dispersed on the carbonaceous support. The average crystallite sizes of ceria in all the catalysts have been estimated by the application of the Scherrer

6

equation [25], and the results are summarized in Table 2. The ceria particle size in Pt/CeO_2 is almost three times larger than those in the activated carbon supported catalysts. No peaks of platinum were observed in the XRD patterns of catalysts, this suggesting that the Pt particles are well dispersed on the catalysts surface.

3.1.4. Temperature-programmed reduction (TPR)

Fig. 2 shows the evolution of H_2 consumption as a function of temperature for the prepared supports. TPR profile of the unsupported CeO_2 includes two broad peaks, at around 785 and 1113 K, associated to the reduction of surface and bulk ceria, respectively [26-28]. In the case of Ce-C supports, all the TPR profiles present a continuous reduction process between 670 and 1120 K, presented as two overlapped shoulders, whose intensities increase with CeO_2 loading. This would indicate a high dispersion of ceria on the carbonaceous support, with a small CeO_2 particle size, facilitating ceria reduction as compared with the bulk ceria support [29].

Fig. 3 shows the temperature-programmed reduction profiles obtained with Pt/Ce-C and Pt/CeO_2 catalysts. The TPR signal for Pt/CeO_2 shows an additional peak centered at 518 K, as compared to the CeO_2 support. According to the literature, this peak at low temperature can be attributed to the reduction of the ceria surface in close contact with the platinum species, together with the reduction of the latter to metallic platinum [24, 30-33]. The second peak, at 730 K, is related to the reduction of surface ceria that is not in close contact with the metal but whose reduction takes place at lower temperatures via H_2 spillover [32, 33]. Indeed, it is well known the ability of noble metals to facilitate the reduction of reducible oxides, such as ceria, via hydrogen spillover, where hydrogen molecules are chemically adsorbed and readily dissociated into atomic species on the surface of the metal. Then, atomic hydrogen spills over to the support surface and easily reacts with the oxide which is in the oxide-metal interface or in the proximity of the latter, promoting the reduction of the oxide at low temperature [24, 34]. Finally, the broad peak appearing around 924 K is related to the bulk reduction of ceria [24,27,35]. Reduction profiles for carbon-supported catalysts show the same feature than Pt/CeO_2, with two overlapping peaks at lower temperatures (356-600 K) and a broad shoulder centered around 845 K.

The appearance of an additional reduction peak at low temperatures along with the peaks shifted toward lower temperatures (in both ceria-supported and carbon-supported catalysts TPR profiles), reveal the presence of an intimate metal-ceria

interaction. This fact promotes the reduction of ceria at lower temperatures through hydrogen spillover from platinum particles towards the support. On the other hand, it can be seen that the use of activated carbon as support of ceria leads to a significant shift in reduction peaks towards lower temperatures with respect to the bulk catalyst. This would indicate a high dispersion of ceria with a larger surface able to interact with the metal particles this enhancing its reducibility via spillover.

3.1.5. X-ray photoelectron spectroscopy (XPS)

Pt 4f level XPS spectra for fresh and reduced Pt/10Ce-C are shown in Fig. 4. In both cases, independently of the applied treatment, platinum spectra exhibit two broad bands, corresponding to the Pt $4f_{7/2}$ and Pt $4f_{5/2}$ levels. Each of these bands can be deconvoluted into two components. The binding energies for the different Pt $4f_{7/2}$ components and their contributions on the signal are reported in Table 3. Fresh catalyst spectrum shows two peaks whose maximum intensities are located at 72.6 and 73.9 eV, that can be assigned to Pt(II) and Pt(IV) respectively, according to the literature [36-38]. The presence of divalent platinum in this catalyst could be due to decomposition of the platinum precursor during support impregnation, involving reduction of Pt(IV) to Pt (II) [39-41]. After reduction at 473 K, a shift of Pt $4f_{7/2}$ band towards lower binding energy can be observed. The peak at 71.5 eV can be attributed to metallic platinum, while the peak appearing at 73.3 eV indicates that a proportion of platinum present in the catalyst remains in oxidized state [36]. Thus, the treatment at 473 K only achieves about 50% of platinum species reduction on the catalyst surface to Pt^0, with higher binding energies for platinum $4f_{7/2}$ transition. This behavior is very consistent with TPR results and could be explained by the presence of platinum-ceria intimate interaction on the catalyst surface, which hinders metal reduction at a lower temperature such as 473 K. The XPS data of the ceria-free catalyst (Pt/C) shown in Table 3 also confirm this fact. Indeed, they show a total reduction of the platinum at 473 K with lower binding energy than for the same catalyst containing ceria (Pt/10Ce-C) affirming that the presence of ceria affects largely the response of platinum to reduction. Furthermore, the presence of residual chlorine inhibits platinum reduction due to formation of stable oxychloroplatinum species (PtO_xCl_y), the reduction of which occurs at higher temperatures than for PtO_x species [42-45].

Superficial composition and cerium oxidation state in the as-prepared and reduced Pt/10Ce-C, obtained by XPS, are reported in Table 3. It can be observed that the

reduction treatment at 473 K produces a slight decrease in the atomic Pt/C and Pt/Ce ratios, which can be considered as an estimation of platinum dispersion on the support. This diminution can be due to a slight sintering of platinum particles during reduction treatment at 473 K. It must be taken into account that the catalyst has not been submitted to any heat treatment prior to reduction. Therefore, it is expected to occur a minor sintering of metal particles during the first heat treatment posterior to the impregnation process. On the other hand, it can be observed that the atomic Ce/C ratio remains unchanged after the reduction treatment, indicating that this treatment does not alter the size of the ceria particles.

XPS analysis also revealed the presence of a considerable amount of chlorine residual species on the catalyst surface. Table 3 reports the Cl/Ce ratios in both the fresh and the reduced catalysts. Chlorine remains on the Pt/10Ce-C surface after reduction at 473 K as it could be expected, since it has been reported in previous works that chlorine is still retained on ceria-based catalyst surface even after reduction treatments at 1173 K [46]. Furthermore, the Cl/Ce ratio increases from 0.3 to 0.5 after reduction of Pt/10Ce-C, indicating chlorine surface enrichment. Similar behavior was observed by Silvestre *et al.* when studying a PtZn/CeO$_2$ catalyst prepared from chlorinated platinum precursor [36]. The authors observed an increase of the chlorine species concentration on the catalyst surface with the reduction temperature, reaching high chlorine enrichment after treatment reduction at 773 K. This enrichment has been related to superficial formation of CeOCl. Several works have reported the presence of such species on the surface of ceria crystals when catalysts were prepared from chlorinated salts [47,48]. Moreover, it has been confirmed that residual chloride anions are highly mobile and can migrate from platinum particles to the support, substituting the oxygen vacancies of ceria, which gives rise to formation of highly stable CeOCl phase [47-50].

In Fig. 4, experimental and fitted Ce3d spectra of fresh and reduced Pt/10Ce-C are shown. The spectra fitting were carried out as has been reported in the literature. It can be seen that there are ten peaks assignments, labeled u and v following the notation established by Burroughs *et al*. [51], related to the 3d$_{3/2}$ and 3d$_{5/2}$ spin-orbit components, respectively. Concretely, v, u, v´´, u´´, v´´´ and u´´´ refer to Ce^{4+} final state, while v$_0$, u$_0$, v´ and u´ correspond to Ce^{3+} final state [50-55]. The degree of ceria reduction was estimated using the following equation [56-58]:

$$\% Ce^{3+} = \frac{[S(u_0) + S(u') + S(v_0) + S(v')]}{\sum [S(u) + S(v)]} \times 100$$

As can be seen in Table 3, the catalyst shows an appreciable amount of Ce^{3+} even in the absence of reduction treatment, which may be related to a photoreduction process of CeO_2 during XPS experiment [53, 57-59]. After reduction at 473 K, the extent of reduced ceria increases from 43 to 50%. This result confirms the presence of an intimate interaction between platinum particles and ceria in this sample, which promotes the reduction of the latter at relatively low temperatures by hydrogen spillover. Moreover, the increase of surface Ce^{+3} can be attributed to formation of CeOCl crystallites on the catalysts surface, according to previous studies [46,50, 60-62]. Thus, Bernal *et al*. [46] evaluated the ceria degree reduction in Rh/CeO_2 catalysts prepared with chlorinated and chlorine-free metallic precursors and observed a high proportion of Ce^{3+} in the chlorinated catalyst after reduction treatment. Furthermore, the authors observed that the extent of reduced ceria varies very slightly with successive evacuation/H_2 adsorption cycles, while the reduction process was reversible for the chlorine-free precursor catalyst. These results have been explained through a ceria lattice oxygen substitution by chloride ions, producing an irreversible reduction of CeO_2. The incorporation of these ions on the oxide surface inhibits both the direct and back spillover processes responsible for the reversibility of ceria reduction by hydrogen.

3.2. Catalytic activity

3.2.1 Toluene hydrogenation

An estimation of the relative platinum dispersion on the prepared catalysts has been performed by evaluating their catalytic activity in the toluene hydrogenation reaction. In the case of the ceria-based catalysts, the usual methods of H_2 and CO chemisorption used to determine metallic dispersion in supported catalysts are unviable because of the ceria ability to adsorb both gases at room temperature [63-65], producing an overestimation of the metal surface exposed [66,67]. Toluene hydrogenation is a structure-insensitive reaction, in which the catalytic activity is exclusively related to the amount of metal atoms exposed on the catalyst surface independently of the metal particle size. However, in spite of the insensitivity to the structure, this reaction can be affected by the presence of electronic effects of partially reduced ceria on the metal particles, generated upon reduction at high temperature. Nevertheless, this effect can be

manifested similarly in both hydrogenation reactions as in the hydrogen chemisorption process [68].

The catalytic activity for toluene hydrogenation at 333 K (as μmol of toluene transformed per gram of Pt) obtained for all catalysts after reduction at 473 K is reported in Table 2. As can be seen, after reduction at 473 K, Pt/10Ce-C shows the best performance in toluene hydrogenation, reaching a much higher activity than all the catalysts. Moreover, the activity of the other prepared catalysts decreases as ceria content increases. Thus, catalyst Pt/CeO_2 shows the lower activity, with 10.6 μmol·s^{-1}·gPt^{-1}. Taking into account the structure-insensitivity of the toluene hydrogenation reaction, this decrease can be related to a lower amount of surface platinum atoms. Also, it can be deduced that Pt/10Ce-C exhibits a high Pt dispersion since it shows a higher activity for toluene hydrogenation than the other catalysts. On the other hand, the low value for the unsupported catalyst activity could be indicative of a low platinum dispersion.

Table 2 also reports the values of catalytic activity for hydrogenation of toluene after reduction at 773 K. An increase in the reduction temperature from 473 to 773 K produces an important decrease in the catalytic activity for all the prepared catalysts, achieving very low values. This behavior is justified by the presence of a strong interaction between the noble metal and ceria particles induced by the reduction at high temperature [27,47,68-71]. In the literature, this interaction has been explained by the presence of electronic effects on the platinum generated by ceria particles partially reduced after high-temperature reduction treatment and which are in contact with it. This interaction changes the metal electronic structure by electronic transfer from ceria, which affects the Pt−toluene bond strength and then hinders the hydrogenation reaction [27,68,72]. These results are in accordance with those of characterization, confirming that metal and ceria particles are in close contact on the surface of these catalysts.

3.2.2. Total oxidation of ethanol

Fig. 5 shows the ethanol conversion and the CO_2 evolution yield as a function of reaction temperature on the evaluated catalysts. It must be mentioned that acetaldehyde, CO_2 and water were the only products formed during the reaction. The Pt/C catalyst exhibits a lower activity and selectivity than ceria-containing supported catalysts, showing that the presence of ceria clearly promotes the oxidation of ethanol. On the other hand, it can be seen clearly that the carbon-supported catalysts show a higher

11

catalytic activity than Pt/CeO_2, which can be due to the high ceria dispersion on the surface of the carbonaceous support. Presence of well dispersed small ceria particles provides a high active surface area, as well as promotes the interaction between ceria and platinum particles, which enhances the catalytic behavior in this reaction. Carbon-supported catalysts show two different behaviors in the investigated temperature range. Thus, at low temperatures the activity of these catalysts increases with decreasing ceria loading. However, in the 398 - 473 K temperature range, the activity order observed is: $Pt/10Ce-C > Pt/20Ce-C > Pt/5Ce-C$, achieving a total ethanol conversion at 398 K, 438 K and 458 K, respectively. These results suggest that the reaction proceeds by two different mechanisms at high and low temperature. On the other hand, total conversion is not reached with Pt/CeO_2 unsupported catalyst in the studied temperature range, showing a conversion of 97.9% at 473 K.

Regarding the selectivity, the carbon-supported catalysts exhibit a considerably higher selectivity to CO_2 than Pt/CeO_2 over the whole temperature range. The catalytic selectivity to CO_2 pursues the following order: $Pt/10Ce-C > Pt/20Ce-C > Pt/5Ce-C > Pt/CeO_2$, reaching a total conversion to CO_2 at 433, 441 and 458 K, respectively. Nevertheless, in the case of the Pt/CeO_2 catalyst, it is only possible to achieve a selectivity to CO_2 of 66.6% at 473 K, for an ethanol conversion of 97.9%.

Catalytic data show that $Pt/10Ce-C$ is the most active and selective of all the prepared catalysts in the total oxidation of ethanol. This sample reaches conversion and selectivity values significantly higher than those obtained for the other catalysts. Moreover it achieves a total ethanol conversion to CO_2 at low temperature. These results agree with those obtained in the toluene hydrogenation reaction, where $Pt/10Ce-C$ shows the highest activity. Therefore, this fact could be related to the high dispersion of platinum particles, which is clearly confirmed by the toluene hydrogenation results. Furthermore, this behavior could be explained by the presence of an optimal interaction between the ceria and highly dispersed platinum particles. This interaction promotes the generation of highly active sites on the catalyst surface and then improves its behavior in the reaction. Indeed, it is well known that metal oxide interaction plays a crucial role in the catalytic oxidation reactions over supported noble metal catalysts on reducible oxides such as ceria. This interaction is enhanced when particles of both, metal and oxide, are small and well dispersed. When an intimate interaction $M-CeO_2$ is achieved, the metal promotes the redox activity of the ceria located at the $M-CeO_2$ interface and thus increases the ceria lattice oxygen mobility and reactivity, which is involved in the

VOCs oxidation through a Mars-van Krevelen mechanism [73-75]. The latter may be the predominant mechanism of the reaction for Pt/Ce-C catalysts but certainly not the only one. In fact, in these catalysts some platinum particles should be found deposited on the carbon support and consequently are isolated from ceria. According to the literature, the reaction of total oxidation of VOCs over these particles usually proceeds through a Langmuir-Hinshelwood mechanism [76, 77].

In order to evaluate the stability of the catalysts during the reaction, an experiment has been performed under extended reaction times using the same reaction conditions. For this purpose, Pt/10Ce-C has been selected as it is the most active catalyst in terms of conversion and selectivity. Fig. 6 shows the evolution of ethanol conversion and the yield to CO_2 at 373 K as a function of reaction time for this catalyst. Practically no deactivation is observed after 100 h, maintaining similar values of ethanol conversion and CO_2 yield during all the experiment. This indicates that Pt/10Ce-C is appropriate for the complete ethanol combustion reaction, in terms of activity/selectivity and stability.

The effect of water vapor on the catalytic activity of the best catalyst, Pt/10Ce-C, has been studied in the ethanol combustion reaction. As it has been mentioned previously, water has been found to act as inhibitor of VOCs oxidation, specially over noble metals catalysts supported on inorganic oxides at low temperatures [78,79]. Thus, the performance of Pt/10Ce-C has been tested under relatively high humidity feed steam conditions, employing a reactant mixture containing 1000 ppm of ethanol in a total air flow of 100 mL·min^{-1} and relative humidity of 40 and 80%. For comparative purposes, the effect of the presence of water vapor on the catalytic behavior of Pt/CeO$_2$ has also been studied. Fig. 7 shows the effect of water vapor concentration on the evolution of ethanol conversion and the yield to CO_2 over the studied catalysts as a function of the reaction temperature. It can be seen that all the conversion profiles shift to higher temperatures in the presence of water vapor, and that this shift enhances with increasing water vapor concentration in the reaction mixture. However, in the case of the carbon-supported catalyst, the conversion decrease is very slight compared with the other sample. In fact, in the absence of humidity this catalyst reaches a total ethanol conversion at 398 K, whereas under relative humidities of 40% and 80%, the temperature of the total conversion is 403 K. On the other hand, the presence of water slightly affects the selectivity of the carbon-supported catalyst, achieving a complete conversion to CO_2 at same temperature of 433 K in the absence of humidity and in the

presence of a high water vapor concentration (RH = 80%). However, the presence of water vapor has a significant negative effect on the selectivity of the Pt/CeO$_2$ catalyst. Moreover, the yield to CO$_2$ on this catalyst decreases with increasing water vapor concentration.

The observed behaviour can be ascribed to a competition of water and ethanol molecules for adsorption on the active sites of the catalysts [76,80]. The coverage of these sites by water molecules leads to a diminution in the amount of active sites available for the oxidation reaction, which results in a decrease of the catalytic activity. The high stability of the carbon-supported catalyst with respect to the ceria-unsupported catalyst can be explained by the hydrophobic character of activated carbon, which prevents water molecules adsorption on the support. This fact results in only a slight decrease of activity. [81-83]. Nevertheless, inorganic supports such as ceria can retain significant amounts of water molecules evolved during combustion, after a competitive adsorption between them and VOCs molecules, which produces a significant decrease in catalytic activity.

3.2.2. Total oxidation of toluene

The evolution of toluene conversion *versus* the reaction temperature for the catalysts is shown in Fig. 8. The reaction products were only CO$_2$ and water. The catalytic activity values follow the same trend as that found in the ethanol oxidation reaction. Consequently, the catalytic activity decreases in the following order: Pt/10Ce-C > Pt/20Ce-C > Pt/5Ce-C > Pt/CeO$_2$, reaching toluene total conversion at 453, 466, 473 and 503 K, respectively. However, the temperatures required for toluene conversion are higher than those observed for ethanol using the same catalysts. Indeed, while Pt/10Ce-C achieves a total conversion of ethanol at 398 K, this temperature is 453 K for toluene total conversion. These results are in agreement with the literature, which reports that toluene total oxidation requires higher temperatures than alcohols [16,17,19,84-87]. Previous studies concluded that the reactivity of VOCs for the total oxidation reaction depends on their functional groups. Thus, the reactivity for these compounds decreases in the following order: alcohols > aromatics > ketones > carboxylic acids > alkanes. These studies related the VOCs reactivity with the strength of C−H bonds, in such a way that those compounds containing C−H single bonds are more reactive and, therefore they are oxidized at lower temperatures [88-90].

14

It should be noted that the conversion values obtained for the ceria-free catalyst (Pt/C) are lower than those of ceria-supported catalysts, confirming the role of the ceria in the reaction of oxidation of VOCs. On the other hand, these results show that the maximum catalytic activity is found for the catalyst containing 10 wt.% in ceria. This indicates that, regardless of the volatile organic compound structure, Pt/10Ce-C exhibits the optimum activity for the total conversion of VOCs among all the catalysts evaluated in this study. As mentioned above, the optimal behavior of this catalyst may be related to the presence of a Pt−CeO$_2$ optimal interface. Thus, the high platinum dispersion along with the presence of small ceria particles on the catalyst surface promotes the establishment of an optimal interaction between both species, which creates highly active sites at the metal-ceria interface.

Finally, it can be concluded that Pt/10Ce-C appears to be efficient in the complete oxidation of VOCs regardless of the compound studied. This catalyst shows a high activity and selectivity towards the final products of the reaction at low temperatures, as well as an excellent stability under the reaction conditions both in the absence and presence of humidity.

4. Conclusions

Platinum catalysts supported on activated carbon and promoted with ceria have been prepared with different ceria loadings and tested in the total oxidation of two representative VOCs, ethanol and toluene. Characterization data have shown that ceria particles are highly dispersed on the surface of the activated carbon support. Moreover, the existence of an intimate interaction between ceria and platinum has been evidenced from the TPR experiments. Toluene hydrogenation has been used as a model reaction to have an estimation of the platinum relative dispersion. Thus, Pt/10Ce-C has exhibited the best performance with a very high hydrogenating activity, which indicates a high platinum dispersion in this catalyst. In the complete oxidation of VOCs, ceria-promoted carbon-supported catalysts have shown higher activity than platinum supported on bulk ceria, both for ethanol and toluene. Furthermore, the most advantageous catalytic performances were found for the catalyst with a 10 wt.% ceria loading, probably due to an optimum synergistic interaction between highly dispersed ceria and platinum particles.

References

[1] J. Williams, R. Koppmann, "Volatile Organic Compounds in the Atmosphere". Edited by Ralf Koppmann, Blackwell Publishing Ltd.: Oxford (2007) 1-19.

[2] D.W.M. Sin, Y.C. Wong, P.K.K. Louis, Atm. Environ. 35 (2001) 5961-5969.

[3] A.J. Kean, E. Grosjean, D. Grosjean, R.A. Harley, Environ. Sci. Technol. 35 (2001) 4198-4204.

[4] R.G. Derwent, M.E. Jenkin, S.M. Saunders, M.J. Pilling, P.G. Simmonds, N.R.Passant, G.J. Dollard, P. Dumitrean, A. Kent, Atmos. Environ. 37 (2003) 1983-1991.

[5] M.M. Galloway, P.S. Chhabra, A.W.H. Chan, J.D. Surratt, R.C. Flagan, J.H. Seinfeld, F.N. Keutsch, Atmos. Chem. Phys. 9 (2009) 3331-3345.

[6] L.F. Liotta, Appl. Catal. B: Env. 100 (2010) 403-412.

[7] F.N. Aguero, A. Scian, B.P. Barbero, L.E. Cadús, Catal. Lett. 128 (2009) 268-280.

[8] L.M. Gandía, M.A. Vicente, A. Gil, Appl Catal B: Env. 38 (2002) 295-307.

[9] S. Scirè, L.F. Liotta, Appl. Catal. B: Env. 125 (2012) 222- 246.

[10] T. Garcia, B. Solsona, D. Cazorla-Amorós, A. Linares-Solano, S.H. Taylor, Appl. Catal. B: Env. 62 (2006) 66-76.

[11] L.M. Petkovic, S.N. Rashkeev, D.M. Ginosar, Catal. Today 147 (2009) 107-114.

[12] H.L. Tidahy, S. Siffert, F. Wyrwalski, J.F. Lamonier, A. Aboukaïs, Cat. Today 119 (2007) 317-320.

[13] F.N. Aguero, A. Scian, B.P. Barbero, L.E. Cadús, Cat. Today 133-135 (2008) 493-501.

[14] B. de Rivas, R. López-Fonseca, C. Jiménez-González, J.I. Gutiérrez-Ortiz, J. Catal. 281 (2011) 88-97.

[15] L. He, Y. Yu, C. Zhang, H. He, J. Environ. Sci. 23 (2011) 160-165.

[16] S. Scirè, P.M. Riccobene, C. Crisafulli, Appl. Catal. B: Env. 101 (2010) 109-117.

[17] S.S.T. Bastos, S.A.C. Carabineiro, J.J.M. Órfão, M.F.R. Pereira, J.J. Delgado, J.L. Figueiredo, Catal. Today 180 (2012) 148-154.

[18] D. Yu, Y. Liu, Z. Wu, Catal. Commun. 11 (2010) 788-791.

[19] D. Delimaris, T. Ioannides, Appl. Catal. B: Env. 89 (2009) 295-302.

[20] A. Trovarelli, Catal. Rev. Sci. Eng. 38 (1996) 439-520.

[21] A. Trovarelli, C. De Leitenburg, M. Boaro, G. Dolcetti, Catal. Today 50 (1999) 353-367.

[22] L. Pino, A. Vita, M. Cordaro, V. Recupero, M.S. Hegde, Appl. Catal. A: Gen. 243 (2003) 135-146.

[23] M.A. Alvarez-Merino, M.F. Ribeiro, J.M. Silva, F. Carrasco- Marín, F.J. Maldonado-Hódar, Environ. Sci. Technol. 38 (2004) 4664-4670.

[24] A. Sepúlveda-Escribano, J. Silvestre-Albero, F. Coloma, F. Rodríguez-Reinoso, Stud. Surf. Sci. Catal. 130 (2000) 1013-1018.

[25] M.R. Gallego, "La difracción de los rayos X" (1982) Ed. Alhambra.

[26] H.C Yao, Y.F.Y. Yao, J. Catal. 86 (1984) 254

[27] A. Sepúlveda-Escribano, F. Coloma, F. Rodríguez-Reinoso, J. Catal. 178 (1998) 649-657.

[28] F. Fally, V. Perrichon, H. Vidal, J. Kaspar, G. Blanco, J.M. Pintado, S. Bernal, G. Colon, M. Daturi, J.C. Lavalley, Catal. Today 59 (2000) 373-386.

[29] J.C. Serrano-Ruiz, A. Sepúlveda-Escribano, F. Rodríguez-Reinoso, D. Duprez, J . Mol. Catal. A: Chem., 268 (2007) 227-234.

[30] A.C.S.F. Santos, S. Damyanova, G.N.R. Teixeira, L.V. Mattos, F.B. Noronha, F.B. Passos, J.M.C. Bueno, Appl. Catal. A: Gen. 290 (2005) 123-132.

[31] E. Rogemond, R. Fréty, V. Perrichon, M. Primet, S. Salasc, M. Chevrier, C. Gauthier, F. Mathis, J. Catal. 169 (1997) 120-131.

[32] R.M. Navarro, M.C. Álvarez-Galván, M. Cruz Sánchez-Sánchez, F. Rosa, J.L.G. Fierro, Appl. Catal. B: Env. 55 (2005) 229-241.

[33] M. Boaro, M. Vicario, J. Llorca, C. de Leitenburg, G. Dolcetti, A. Trovarelli, Appl. Catal. B: Env. 88 (2009) 272-282.

[34] Z-Q. Zou, M. Meng, Y-Q. Zha, J. Phys. Chem. C 114 (2010) 468-477.

[35] R. Buitrago, J. Ruiz-Martínez, J. Silvestre-Albero, A. Sepúlveda-Escribano, F. Rodríguez-Reinoso, Catal. Today 180 (2012) 19-24.

[36] J. Silvestre-Albero, F. Coloma, A. Sepúlveda-Escribano, F. Rodríguez-Reinoso, Appl. Catal. A: Gen. 304 (2006) 159-167.

[37] A. Huidobro, A. Sepúlveda-Escribano, F. Rodríguez-Reinoso, J. Catal. 212 (2002) 94-103.

[38] P. Bera, K.R. Priolkar, A. Gayen, P.R. Sarode, M.S. Hegde, S. Emura, R. Kumashiro, V. Jayaram, G.N. Subbanna, Chem. Mater. 15 (2003) 2049-2060.

[39] H.E. Van Dam, H. Van Bekkum, J. Catal. 131 (1991) 335-349.

[40] F. Coloma, A.sepúlveda-Escribano, J.L.G. Fierro, F.Rodríguez-Reinoso, Langmuir 10 (1994) 750-755.

[41] F. Coloma, A. Sepúlveda-Escribano, J.L.G. Fierro, F. Rodriguez-Reinoso, Appl. Catal. A. Gen. 148 (1996) 63-80.

[42] M. Paulis, H. Peyrard, M. Montes, J. Catal. 199 (2001) 30-40.

[43] H. Lieske, G. Lietz, H. Spindler, J. Völter, J. Catal. 81 (1983) 8-16.

[44] E. Marceau, M. Che, J. Saint-Just, J.M. Tatibouët, Catal. Today 29 (1996) 415-419.

[45] C. Contescu, D. Macovei, C. Craiu, C. Teodorescu, J.A. Schwarz, Langmuir 11 (1996) 2031-2040.

[46] S. Bernal, J.J. Calvino, G.A. Cifredo, J.M. Gatica, J.A. Pérez Omil, A. Laachir, V. Perrichon, Stud. Surf. Sci. Catal. 96 (1995) 419-429.

[47] L. Kępiński, M. Wołcyrz, J. Okal, J. Chem. Soc., Faraday Trans. 91 (1995) 507-515.

[48] L. Kępiński, J. Okal, J. Catal. 192 (2000) 48-53.

[49] F.J. Gracia, J.T. Miller, A.J. Kropf, E.E.Wolf, J. Catal. 209 (2002) 341-354.

[50] F.L. Normand, L. Hilaire, K. Kili, G. Krill, G. Maire, J. Phys. Chem. 92 (1988) 2561-2568.

[51] P. Burroughs, A. Hammett, A.F. Orchard, G.J. Thornton, J. Chem. Soc. Dalton Trans. 17 (1976) 1686-1698.

[52] M. Romeo, K. Bak, J. El Fallah, F. Le Normand, L. Hilaire, Surf. Interf. Anal. 20 (1993) 508-512.

[53] M.S.P. Francisco, V.R. Mastelaro, P.A.P. Nascente, A.O. Florentino, J. Phys. Chem. B 105 (2001) 10515-10522.

[54] J.Z. Shyu, W.H. Weber, H.S. Gandhi, J. Phys. Chem. 92 (1988) 4964-4970.

[55] N. Thromat, M. Gautier-Soyer, G. Bordier, Surf. Sci. (1996) 290-302.

[56] A. Laachir, V. Perrichon, A. Badri, J. Lamotte, E. Catherine, J.C. Lavalley, J. El Fallah, L. Hilaire, F. Le Normand, E. Quéméré, G.N. Sauvion, O. Touret, J. Chem. Soc., Faraday Trans. 87 (1991) 1601-1609.

[57] M. Daturi, C. Binet, J.C Lavalley, A. Galtayries, R. Sporken, Phys. Chem. Chem Phys. 1 (1999) 5717-5724.

[58] G. Dong, J. Wang, Y. Gao, S. Chen, Catal. Lett. 58 (1999) 37-41.

[59] A. Trovarelli, F. Zamar, J. Llorca, C. de Leitenburg, G. Dolcetti, J. T. Kiss, J. Catal. 169 (1997) 490-502.

[60] S. Salasc, V. Perrichon, M. Primet, M. Chevrier, F. Mathis, N. Moral, Catal. Today 50 (1999) 227-235.

[61] C. Force, J.P. Belzunegui, J. Sanz, A. Martínez-Arias, J. Soria, J. Catal. 197 (2001) 192-199.

[62] A. Bensalem, F. Bozon-Verduraz, V. Perrichon, J. Chem. Soc. Faraday Trans. 91 (1995) 2185-2189.

[63] V. Perrichon, L. Retailleau, P. Bazin, M. Daturi, J.C. Lavalley, Appl. Catal. A: Gen. 260 (2004) 1-8.

[64] S. Bernal, J.J. Calvino, G.A. Cifredo, J.M. Gatica, J.A. Pérez Omil, J.M. Pintado, J. Chem. Soc., Faraday Trans. 89 (1993) 3499-3505.

[65] J.L.G. Fierro, J. Soria, J.Solid State Chem. 66 (1987) 154-162.

[66] S. Bernal, J.J. Calvino, G.A. Cifredo, J.M. Rodríguez-Izquierdo, V. Perrichon, A. Laachir, J. Chem. Soc., Chem. Commun. (1992) 460-462.

[67] S. Bernal, J.J. Calvino, G.A. Cifredo, J.M. Rodríguez-Izquierdo, V. Perrichon, A. Laachir, J. Catal. 137 (1992) 1-11.

[68] J. Silvestre-Albero, F. Rodríguez-Reinoso, Sepúlveda-Escribano, J. Catal. 210 (2002) 127-136.

[69] S. Bernal, F.J. Botana, J.J. Calvino, M.A. Cauqui, G.A. Cifredo, A. Jobacho, J.M. Pintado, J.M. Rodríguez-Izquierdo, J. Phys. Chem. 97 (1993) 4118-4123.

[70] P.N.Da Silva, M. Guenin, C. Leclercq, R. Frety, Appl. Catal. 54 (1989) 203-215.

[71] P. Meriaudeau, J.F. Dutel, M. Dufaux, C. Naccache, Stud. Surf. Sci. Catal. 11 (1982) 95-104.

[72] J.C. Serrano-Ruiz, J. Luettich, A. Sepúlveda-Escribano, F. Rodríguez-Reinoso, J. Catal. 241 (2006) 45-55.

[73] S. Scirè, S. Minicò, C. Crisafulli, C. Satriano, A. Pistone, Appl. Catal. B: Env. 40 (2003) 43-49.

[74] M.A. Centeno, M. Paulis, M. Montes, J.A. Odriozola, Appl. Catal. A: Gen. 234 (2002) 65-78.

[75] P. Bera, K.C. Patil, V. Jayaram, G.N. Subbanna, M.S. Hegde, J. Catal. 196 (2000) 293-301.

[76] S. Morales-Torres, A.F. Pérez-Cadenas, F. Kapteijn, F. Carrasco-Marín, F.J. Maldonado-Hódar, J.A. Moulijn, Appl. Catal. B: Env. 89 (2009) 411-419.

[77] J. Bedia, J.M. Rosas, J. Rodríguez-Mirasol, T. Cordero, Appl. Catal. B 94 (2010) 8-18.

[78] K. Persson, L.D. Pfefferle, W. Schwartz, A. Ersson, S.G. Jaras, Appl. Catal. B: Env. 74 (2007) 242-250.

[79] P. Papaefthimiou, T. Ioannides, X.E. Verykios, Appl. Catal. B: Env. 15 (1998) 75-92.

[80] H. Pan, M. Xu, Z. Li, S. Huang, C. He, Chemosphere, 76 (2009) 721-726.

[81] J.C.S. Wu, Z.A. Lin, F.M. Tsai, J.W. Pan, Catal. Today 63 (2000) 419-426.

[82] M. Zhang, B. Zhou, K.T. Chuang, Appl. Catal. B: Env. 13 (1997) 123-130.

[83] A.F. Pérez-Cadenas , S. Morales-Torres , Francisco J. Maldonado-Hódar, F. Carrasco-Marín, Appl. Catal. A: Gen. 366 (2009) 282-287.

[84] S. Scirè, S. Minicò, C. Crisafulli, S. Galvagno, Catal. Commun. 2 (2001) 229-232.

[85] J. Hermia, S. Vigneron, Catal. Today 17 (1993) 349-358.

[86] E. Noordally, J.R. Richmond, S.F. Tahir, Catal. Today 17 (1993) 359-366

[87] R. Bonelli, S. Albonetti, V. Morandi, L. Ortolani, P.M. Riccobene, S. Scirè, S. Zacchini, Appl. Catal. A: Gen. 395 (2011) 10-18.

[88] A. Schwartz, L.L. Holbrook, H. Wise, J. Catal. 21 (1971) 199-207.

[89] V.D. Sokolovskii, Catal. Rev.-Sci. Eng. 32 (1990) 1-49.

[90] A. O'Malley, B.K. Hodnett, Catal. Today 54 (1999) 31-38.

Table

Table 1. Textural properties of the supports

Sample	S_{BET} $(m^2 \cdot g^{-1})$	V_0 $(cm^3 \cdot g^{-1})$	V_{meso} $(cm^3 \cdot g^{-1})$
AC	1525	0.51	0.65
5Ce-C	1428	0.48	0.59
10Ce-C	1324	0.45	0.53
20Ce-C	1126	0.40	0.45
CeO_2	124	0.01	0.05

Table 2. Metal content, CeO_2 crystallite size and catalytic activity for toluene hydrogenation of the catalysts

Catalyst	Pt(wt.%)[a]	CeO_2 (wt.%)[a]	D_{CeO2} (nm)[b]	Activity $(\mu mol \cdot s^{-1} \cdot gPt^{-1})$[c]	
				Red. 473 K	Red. 773 K
Pt/5Ce-C	0.82	3.97	5.1	30.9	0.6
Pt/10Ce-C	0.89	7.28	4.8	137.8	0.3
Pt/20Ce-C	0.85	13.18	5.1	24.3	0.5
Pt/CeO_2	1.09		13.7	10.6	0.1

[a] Determined by ICP-OES.
[b] Estimated from the (111) ceria diffraction peak using Scherrer equation.
[c] Reaction temperature: 333 K, H_2 flow: 50 ml.min^{-1}, H_2/C_7H_8 ratio: 36.

Table 3. Pt/C and Pt/10Ce-C catalysts characterization by XPS

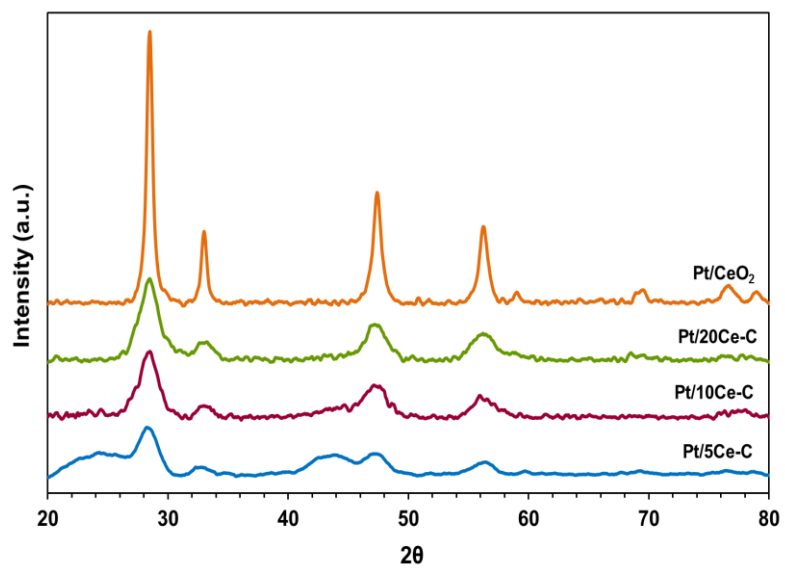| Catalyst	T Red (K)	BE Pt $4f_{7/2}$ (eV)	Pt/C	Pt/Ce	Ce/C	Cl/Ce	Ce^{3+}(%)
Pt/C	-	73.8 (100%)	0.0006	-	-	-	-
	473	71.8 (100%)	0.0003	-	-	-	-
Pt/10Ce-C	-	72.6 (64.6%) 73.9 (35.4%)	0.0007	0.06	0.01	0.3	43.3
	473	71.5 (54.2%) 73.3 (45.8%)	0.0005	0.04	0.01	0.5	50.0

Figure

Fig. 1. X-ray diffraction patterns of Pt/Ce-C and Pt/CeO$_2$ catalysts.
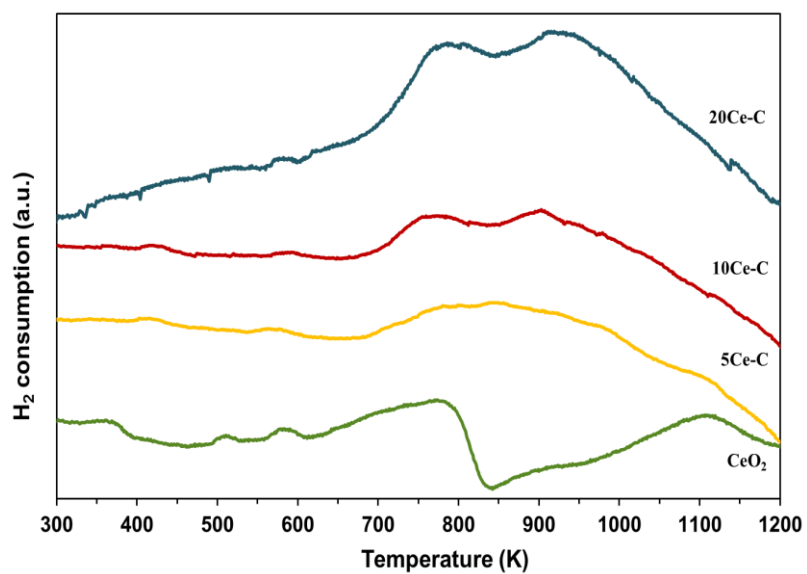

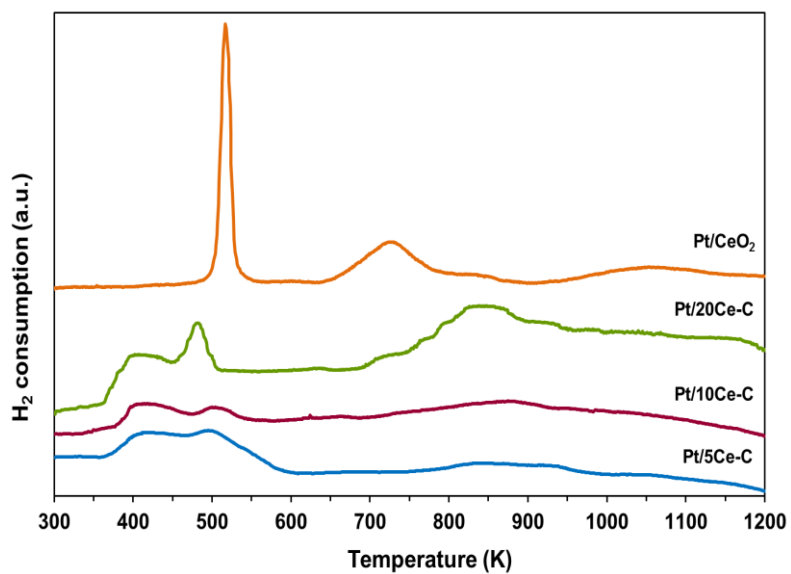Fig. 2. TPR curves (H$_2$ consumption) for Ce-C and CeO$_2$ supports.

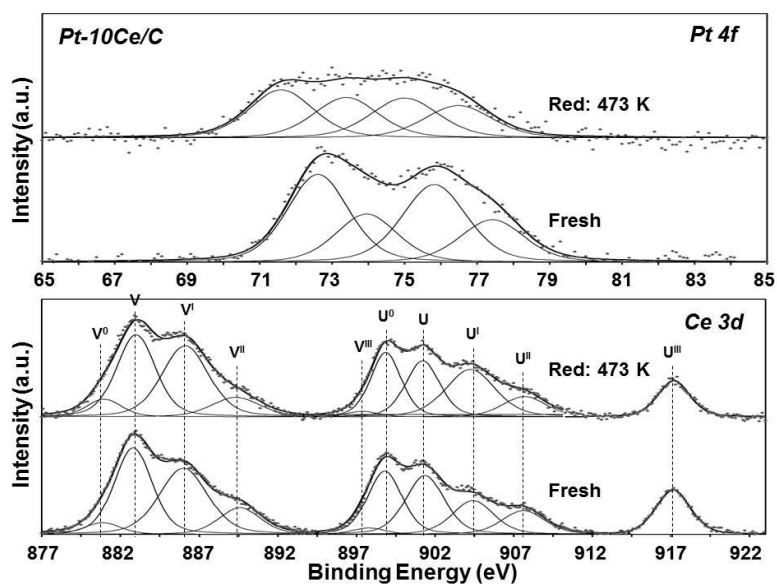Fig. 3. TPR profiles of the Pt/Ce-C and Pt/CeO$_2$ catalysts.

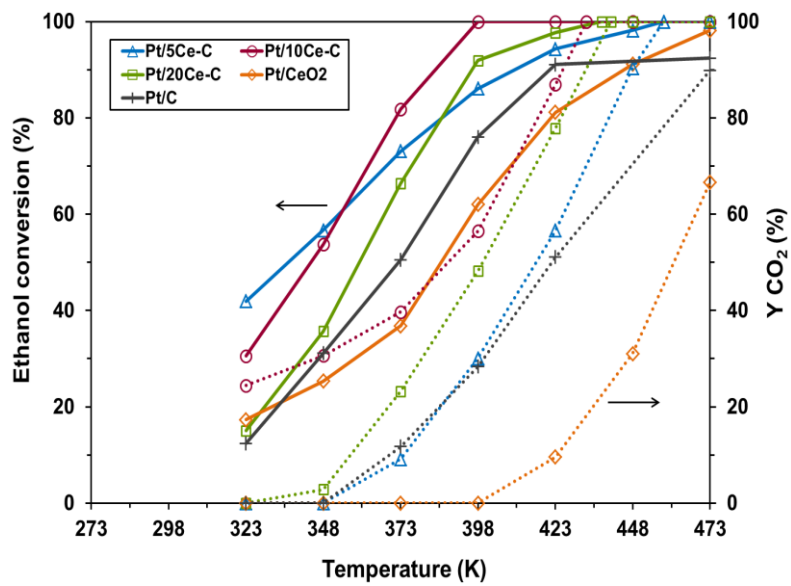Fig. 4. XPS Pt 4f and Ce 3d spectra of the as-prepared and reduced Pt/10Ce-C catalyst.

Fig. 5. Ethanol conversion as a function of reaction temperature for all catalysts. Reaction conditions: 1000 ppm ethanol, 100 ml.min^{-1} air flow, reduction in situ at 473 K (1h, 50 ml.min^{-1} of H_2).
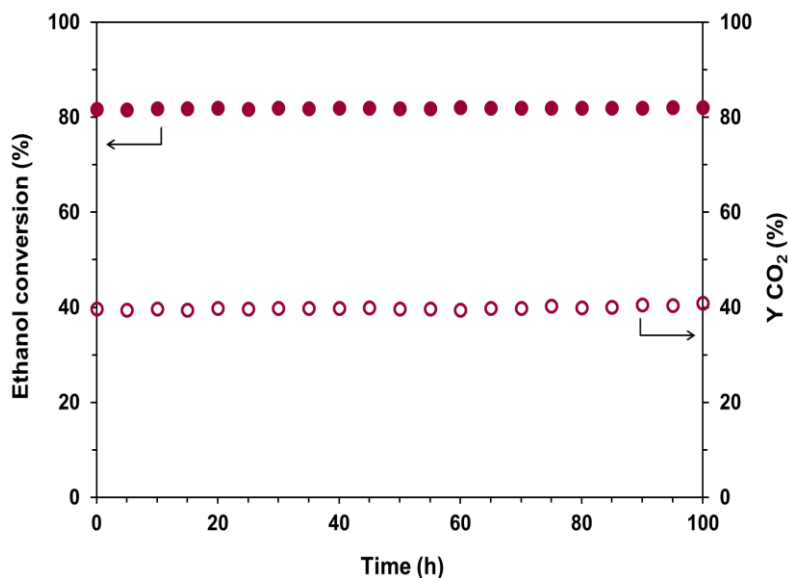
Fig. 6. Stability test for Pt-10Ce/C catalyst at 373 K (1000 ppm ethanol, 100 ml.min^{-1} air flow, reduction in situ at 473 K (1h, 50 ml.min^{-1} of H_2).
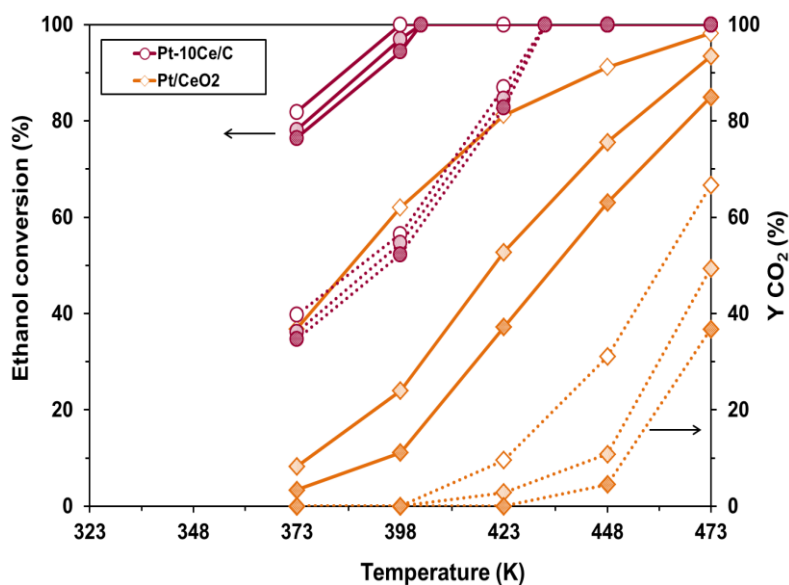

Fig. 7. Conversion of ethanol and yield to CO_2 for Pt/10Ce-C (RH=0% ‒o‒, RH=40% ‒⊗‒ and RH=80% ‒●‒) and Pt/CeO$_2$ (RH=0% ‒◇‒, RH=40% ‒◈‒ and RH=80% ‒◆‒) catalysts. Reaction conditions: 1000 ppm ethanol, 100 ml.min^{-1} air flow, reduction at 473 K (1h).
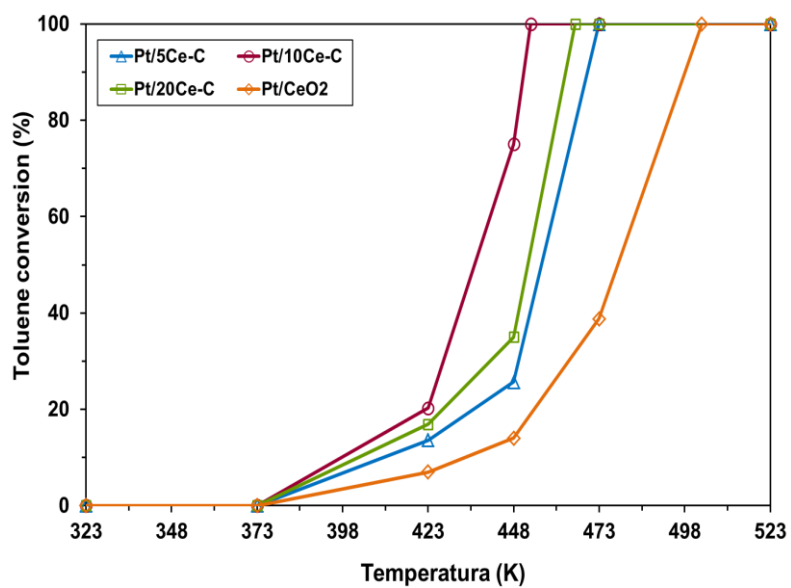
Fig. 8. Toluene conversion as a function of reaction temperature for all the catalysts. Reaction conditions: 1000 ppm toluene, 100 ml.min^{-1} air flow, reduction at 473 K (1h).